Published in final edited form as:

Ann Plast Surg. 2014 June ; 72(0 2): S176–S183. doi:10.1097/SAP.0000000000000107.

Osteoinduction of Umbilical Cord and Palate Periosteum-Derived Mesenchymal Stem Cells on Poly-Co-Glycolytic Acid Nano-Microfibers

Montserrat Caballero, PhD[1], **Andrew Pappa, BS**[1], **Katherine Roden, BS**[1], **Daniel J. Krochmal, MD**[1], and **John A. van Aalst, MD, MA, FACS, FAAP**[1,*]

[1]Division of Plastic & Reconstructive Surgery, Department of Surgery, University of North Carolina, Chapel Hill, NC

Abstract

The need for tissue engineered bone to treat complex craniofacial bone defects secondary to congenital anomalies, trauma, and cancer extirpation is sizeable. Traditional strategies for treatment have focused on autologous bone in younger patients and bone substitutes in older patients. However, the capacity for merging new technologies, including the creation of nano and microfiber scaffolds with advances in natal sources of stem cells, is crucial to improving our treatment options. The advantages of using smaller diameter fibers for scaffolding are two-fold: the similar fiber diameters mimic the *in vivo* extracellular matrix construct;, and smaller fibers also provide a dramatically increased surface area for cell-scaffold interactions. In this study, we compare the capacity for a polymer with Federal Drug Administration (FDA) approval for use in humans, poly-co-glycolytic acid (PLGA) from Delta polymer, to support osteoinduction of mesenchymal stem cells (MSCs) harvested from the umbilical cord (UC) and palate periosteum (PP). Proliferation of both UC- and PP-derived MSCs was improved on PLGA scaffolds. PLGA scaffolds promoted UC MSC differentiation (indicated by earlier gene expression and higher calcium deposition), but not in PP-derived MSCs. UC-derived MSCs on PLGA nano-micro-fiber scaffolds have potential clinical utility in providing solutions for craniofacial bone defects, with the added benefit of earlier availability.

Keywords

Tissue engineering; bone; PLGA; nanofibers; mesenchymal stem cells

Introduction

Craniofacial bone defects are a significant cause of infant morbidity, with significant lifetime functional, esthetic, and social consequences.[1, 2] Effective repair of these defects represents a challenging problem, requiring extensive surgical procedures, generally staged

*Corresponding Author Information: John A. van Aalst, Department of Surgery, Division of Plastic Surgery, 7033 Burnett-Womack Building, CB7195, Chapel Hill, NC 27599-7195, Phone: (919) 843-1087, Fax: (919) 966-3814, john_vanaalst@med.unc.edu.

This manuscript was presented at the 56th Annual Meeting of the Southeastern Society of Plastic and Reconstructive Surgeons, and was winner of the Resident Competition Award. June 1–5, 2013. Bonita Springs, FL, USA.

from infancy through adulthood. The most common treatment for craniofacial defects is autologous bone grafting. Complications for autografts are as high as 30% and include donor site morbidity, pain, infection, and hematoma; an ever-present concern is limited availability of donor material.[3–5] Tissue engineering constitutes a promising approach to overcome current treatment limitations.[6–8] Primary requirements for bone engineering include a biocompatible and biodegradable scaffold to provide temporary mechanical support, an autologous cell source that is readily and reliably available with the capacity to fill the defect.

High surface area nano-micro-fibers (NMF) [9] can be created from multiple natural and synthetic materials,[10–12] providing 3-dimensional scaffolds that mimic the extracellular matrix (ECM) and promote cellular adherence, proliferation and migration.[13, 14] The ECM has fibers with a wide range of diameters, and include collagens (generally 10–500 nm) and elastin fibrils (100–200 nm) depending on tissue structure, location, and age. In most tissues, collagen fibrils are packed in wider fibers with diameters 1–20 μm. Elastic fibrils are usually found packed in wider fiber networks with diameters of 0.2–1.5 μm.[15] Because of this variety in fiber sizes, NMF with variations in size will most closely mimic the ECM.

NMF can be created using several techniques, the most common of which is electrospinning (Figure 1).[10] Though the polymers available for electrospinning are numerous, the use of materials with proven implantation histories would be valuable. Individual polymers used in resorbable plating systems have been used to create nanofibers, and include poly-L-lactic acid (PLA), and poly-lactic-co-glycolytic acid (PLGA);[11][16] however, there are no reports in the literature of any patented resorbable plating systems used for NMF creation. In this study, we use the Delta System™ from Stryker® (Kalamazoo, Michigan, USA) to electrospin NMF.

There are multiple possibilities for mesenchymal stem cell (MSC) sources in pediatric patients, one of which, the umbilical cord (UC), has been significantly underutilized to date. The UC is discarded, and may represent the largest untapped source of embryonic-like MSCs.[17, 18] Another theoretical source of stem cells would be any routinely encountered tissue at the time of a surgical procedure. In adults, lipoaspirate and abdominoplasty specimens with fat have been utilized in this manner.[19]However, in children, there are no surgical procedures that routinely discard large quantities of fat. There are however, other procedures, where the periosteal layer (a rich site of MSCs) are routinely exposed,[20–22] including cleft lip repair (3 months-of-age), cranial vault reconstruction (6 months-of-age) or palate repair (9 to 12 months-of-age). The periosteal layer is known to promote bone healing, as well as prevent desiccation and infection of underlying bone, in part because of the multi-potential MSCs. These MSCs may not have the embryonic-like characteristics of UC MSCs,[23] but could have significant value in tissue engineered bone for children.[22] We have previously demonstrated that UC MSCs appear to have a higher capacity for osteoinduction than PP MSCs. A potential explanation for this is that UC MSCs may be more primitive and hence more plastic, resulting in increased osteoinduction potential.[23]

In this study we report the capacity of poly (lactic-*co*-glycolic acid) (PLGA; Delta System™ polymer resorbable craniofacial plates and screws) to support osteoinduction of MSCs harvested from two different sources, the human umbilical cord and palate periosteum.

Materials and Methods

Electrospinning Nano-micro-fibers

To generate NMF scaffolds, Delta System™ resorbable implants (PLGA) from Stryker® (Kalamazoo, Michigan, USA) were solubilized in 3:1v/v dichloromethane:dimethyl formamide at 8% wt/v concentration, and electrospun at 4.4 kV/inch, CO_2 flow rate of 1 l/min, and polymer flow rate of 0.1 ml/hr (Figure 1). NMF were visualized by scanning electron microscopy (SEM) to determine fiber uniformity (Figure 2). Fibers were sterilized in 70% ethanol under the UV lamp for 4 hours, and incubated with media overnight to facilitate cell attachment.

NF diameter and pore size distribution

Fiber images were obtained on a Hitachi S-3200N environmental SEM. To determine fiber diameter distribution, the ASTM D 629 and AATCC Test Method 20A for fiber counting in microscopic analysis was adapted from industry standard methods. Briefly, 4–5 SEM images were taken randomly from each sample with a magnification range (1000–2000X). Fiber diameters were measured in each image starting at the center of the image's left edge and moving in the horizontal direction to the center of the right edge. Fiber diameters were measured by moving vertically from the top edge center to the bottom edge center of the image. The fiber diameter measurements from all the images (4–5 per sample) were then combined for analysis. A total of 150–200 fibers were analyzed for each of the samples. Pore size distributions were measured with quasi-2D layers of fibers only 2 to 4 fiber diameters thick. SEMs were obtained with sufficient contrast to allow further image manipulations. SEM images of these layers were converted to black-and-white images with appropriate thresholds. Pore size region recognition and area measurements were performed on the converted images using ImageJ software.[24]

Umbilical Cord MSC Harvest

Following Institutional Review Board approval, UC MSCs were harvested using an explant technique, as previously described.[23] Briefly, UC were obtained following appropriate consent (IRB: 06-0801), the blood vessels were discarded, and the remaining Wharton's Jelly and surrounding tissue were cut into small explants and cultured in DMEM/F12 with 10% fetal bovine serum (FBS). The isolated UC-derived MSCs were confirmed negative for CD34 and positive for SSEA-4, CD73, CD90, and CD105.[25–27]

Palatal Periosteum MSC Harvest

Following IRB approval, PP MSCs were harvested from children undergoing cleft palate repair using an explant technique as previously described. [11, 23] Four mm^2 punch biopsies were cut into small explants, and cultured in DMEM/F12 with 10% FBS. Surface markers utilized for identification of MSC origin were similar to UC MSCs.[23, 25]

Flow cytometry

To test for MSC surface markers, UC and PP MSC were analyzed by flow cytometry.[23] Passage 1 cells were resuspended in cold blocking buffer (0.5% BSA, 0.01% Na azide in PBS). Cells were treated with conjugated primary antibody for 20 mn on ice, washed with cold PBS, fixed in 1% paraformaldehyde, and analyzed in a Beckman-Coulter (Dako, Carpinteria, CA, USA) CyAn ADP using the Summit 4.3 software.

Osteoinduction

Passage 2 or 3 MSCs were seeded onto regular tissue culture plates (2-D) or PLGA scaffolds at a density of 4×10^4 cells/cm^2. Cells were then differentiated in α-MEM medium supplemented with 10% FBS, 2mM glutamine, 0.1μM dexamethasone, 50 μM ascorbic acid, 10mM β-glycerophosphate, with media changes every 3 days. Cultures were assayed at days 1, 3, 7, 14 and 21 for cell viability, proliferation and osteogenic differentiation.

Cell proliferation

DNA quantification was used to evaluate cell proliferation. At the different time points, cells were lysed in 10 mM Tris/HCl pH 8.0, 1 mM EDTA, 1% SDS and digested overnight at 55°C with 0.5 mg/ml proteinase K; enzyme was inactivated for 5 minutes at 95°C. The DNA content of the samples was quantitated using the Quant-iT dsDNA BR Assay (Invitrogen, Grand Island, NY, USA).

Cell Viability

To evaluate cell viability, cultures were washed in PBS and stained with green-fluorescent calcein-AM and red-fluorescent ethidium homodimer-1, using the LIVE/DEAD® Viability/ Cytotoxicity assay (Invitrogen, Grand Island, NY, USA). Fluorescence staining was visualized by fluorescence microcopy using a Nikon Eclipse Ti-S inverted microscope.

Alizarin Red S staining

To demonstrate the presence of insoluble calcium deposition, the osteoinduced cells were fixed in 10% buffered formalin for 30 minutes and rinsed with distilled water. Cells were stained with 2% Alizarin Red S solution at pH 4.2 for 10 minutes with gentle agitation. Cells were then washed with distilled water to remove excess dye, followed by tap water. The Alizarin Red S staining was analyzed under light microscopy using a Nikon Eclipse Ti-S inverted microscope.

Alizarin Red quantification

For quantification of staining, Alizarin Red was extracted with 10% (v/v) acetic acid for 30 minutes at room temperature with shaking. After incubation, the cell monolayer with acetic acid was transferred to a 1.5-mL microcentrifuge tube and vortexed for 30 sec. The solution was then overlaid with mineral oil, heated at 85°C for 10 min, and transferred to ice for 5 min. Samples were then centrifuged at 20,000g for 15 min and the supernatant was mixed with 10% (v/v) ammonium hydroxide (5:2) to neutralize the acid (final pH= 4.1–4.5). Samples were read in triplicate at 405 nm.

RT-PCR analysis

To analyze expression of genes involved in MSC osteogenic differentiation, the total cellular RNA was isolated using the RNeasy total RNA extractionkit from Qiagen (Gaithersburg, MD, USA). Real-time fluorescent quantitative PCR was performed by using an ABI PRISM 7700 (Applied Biosystems, Grand Island, NY, USA) using specific primers sequence for the listed genes (Table 1). The ribosomal 18S RNA was used as an internal standard and the $2^{-\Delta\Delta CT}$ quantification method was used for data analysis.

Statistical analysis

Experiments were run in duplicate using at least four different cell lines to account for individual variations. Values are reported as mean ± standard error of the mean of four independent experiments. Statistical analyses were performed using GraphPad Prism 5®. A two-way analysis of variance (ANOVA) test was used to determine significant differences between groups. Comparison between means was determined using the Bonferroni post-hoc test using a confidence level of 0.05.

Results

Scaffold diameter and porosity

PLGA polymer was successfully electrospun into homogenous scaffolds (Figure 2). Using electron microscopy, mats were noted to contain a mixture of nano and micro fibers with diameters ranging from 0.6 to 2.1 μm. Pore size distribution was homogenous, and predominantly distributed between 0–6 μm.

Characterization of MSCs

Both populations of stem cells were negative for CD34 and demonstrated appropriate surface markers for MSCs by flow cytometry (Figure 3). PP MSCs demonstrated significantly lower levels of SSEA-4 and CD90, as previously reported,[23] and may be an indication of greater pre-commitment of the periosteal-derived stem cells.

Proliferation and viability of MSCs on 2D and MNF surfaces

UC MSCs demonstrated an earlier increase in proliferation (day 3) for the PLGA condition vs. the 2D culture (day 7). From day 3 onward, the PLGA NMF condition demonstrated greater viability than the 2D condition (Figure 4). Declining cell proliferation was noted by day 14 for PLGA conditions. Cell viability was maintained throughout the 14-day experiments in both 2D and PLGA conditions.

Proliferation of PP MSCs increased by day 7 in 2D cultures and day 3 for PLGA; higher proliferation rates were noted compared to UC MSCs. Unlike UC MSCs, PP MSC proliferation started to decline at day 14 for both 2D and PLGA conditions. Direct comparison of proliferation between UC and PP MSCs, suggests that PP proliferation is higher in 2D cultures compared to UC at days 3 and 7 (Table 2). PLGA scaffold-induced proliferation was similar for both PP and UC cells. Viability was lower for PP than UC MSCs in all conditions. There seemed to be a correlation between earlier cell proliferation and earlier decrease in viability.

Calcium deposition during differentiation of MSCs

All osteoinduced conditions for both PP and UC MSCs demonstrated the presence of calcium deposition (Figure 5). In UC MSCs, calcium deposition was first detected at day 7 and increased until day 14 for all conditions. Calcium deposition was higher for all NMF scaffold than for 2D conditions. In PP MSC osteoinduction, calcium deposition was initially detected at day 7, and increased until day 14 for 2D conditions, but not for PLGA-supported conditions. Calcium deposition remained higher in 2D cultures than NMF scaffolds for days 14. PP MSCs demonstrated greater calcium deposition at days 14 than did UC MSCs. UC MSC differentiation however demonstrated higher calcium deposition on NMFs than PP (Table 2).

Analysis of gene expression during MSC differentiation

In UC MSCs, bone morphogenic protein-2 (BMP2) expression increased over time until day 14 for 2D cultures. PLGA-supported cultures demonstrated similar increased expression until day 14 (Figure 6, Table 3). Alkaline phosphatase (ALP) mRNA increased over time in all three conditions. Although not significant, there was a higher expression at day 3 in 2D cultures compared to the NMF-supported cultures.

In PP MSC osteoinduction, BMP2 mRNA increased in 2D cultures until day 14. PP MSCs differentiated on PLGA demonstrated a minor increase in BMP2 expression until day 14, similar to UC-derived MSCs.

ALP mRNA mirrored BMP2 expression, demonstrating an increase over time in 2D cultures. No increase was noted in PLGA-supported conditions. Osteocalcin (OTC) mRNA increased by day 7 and continued until day 14 for cells seeded on 2D surfaces. An increase was also detected for PLGA by day 14. Levels of OTC expression increased by day 14 in PLGA conditions and were comparable to 2D levels. Osteopontin (OPN) mRNA expression in PP MSCs increased at day 14 on 2D surfaces (Figure 7, Table 3).

Discussion

Strategies focused on tissue-engineered bone constitute a promising approach to overcome current limitations in the surgical repair of craniofacial bone defects (limited graft supply and the need for a secondary surgical site with attendant morbidities). In this study, we have demonstrated that Stryker® resorbable Delta System™ can be electrospun reliably into a combination of nanofibers and microfibers that mimic the ECM. These NMF scaffolds provide a 3D surface for umbilical cord and palate periosteum MSC attachment, proliferation, and osteoinduction.

In comparing MSCs from the two sources, we have noted that UC and PP MSCs possess comparable surface markers (confirming their mesenchymal identity), with the exception of CD90 and SSEA-4.[23] CD90 levels were lower in PP MSCs; because lower expression of CD90 is an indication of a more differentiated state along a continuum of osteogenic lineage, this is likely an indication that PP MSCs have a greater initial commitment to an osteogenic lineage.[28, 29] Clinically, this appears logical because the role of periosteal MSCs is to provide a source of bone healing following injury.[30] The higher percentage of

UC MSCs with the surface marker SSEA-4, previously thought to be limited to embryonic stem cells,[31] but more recently demonstrated on MSCs,[27, 32] is likely an indication that UC MSCs are more primitive than those from the periosteum, and hence less committed to an osteogenic lineage.

While both UC and PP MSCs were successfully osteoinduced, there was a qualitative increase in osteogenic specific gene expression (in particular, BMP2) and calcium deposition in UC MCSs. This increase was not detected in osteoinduced PP MSCs, which conversely appeared to demonstrate improved differentiation on 2D surfaces. Stem cells that possess characteristics of later stage osteogenic differentiation (e.g. PP MSCs) appear to die in a few days under standard tissue culture conditions, in comparison to cultures of cells at an earlier differentiation stage (consistent with the UC MSCs).[33] In our study, the correlation between earlier differentiation and a shorter time period of viability for PP MSCs when compared to UC MSCs supports this hypothesis.[33] Decrease in viability is even more pronounced in nanofiber-supported conditions, correlating with an accelerated differentiation into the osteogenic lineage with earlier appearance of late stage markers for PP MSCs under these conditions. Our tentative conclusion is that NMF scaffolds induce earlier differentiation in both sets of MSCs. Because the PP MSCs are already further along in the osteogenic continuum, they complete this differentiation process sooner, and hence lose viability sooner.

BMP2 and ALP are considered early markers in bone differentiation,[34] while OTC is an indication of a more mature osteoblastic phenotype and terminal differentiation.[35]BMP2 is involved in bone differentiation and regulates transcription of other osteogenic genes, in particular, increasing the expression of both ALP and OTC. BMP2 mRNA increased as early as day 3 for both UC and PP MSCs, followed by an increase in ALP, OTC, with calcium deposition in the extracellular matrix, all of which is consistent with what is known about BMP2 function.[34,35]

Osteogenic differentiation of PP MSCs starts earlier than in UC MSCs, with 2D cultures showing higher BMP2 and higher calcium deposition by day 7. This is explained by the fact that PP MSCs are already preconditioned toward an osteogenic lineage; earlier differentiation capacity is supported by a lower CD90 surface marker distribution in PP MSCs described earlier. While PP MSC differentiation is poorer on PLGA NMFconditions, fiber scaffolds increased UC MSC differentiation to levels comparable to PP MSCs in 2D conditions. MSC differentiation on PLGA-supported conditions begins earlier than 2D conditions with demonstration of higher levels of BMP2 and calcium deposition.

Another protein marker of osteogenesis is OPN, which is produced by pre-osteoblasts, mature osteoblasts, and osteocytes.[33] We detected an increase over time in OPN for PP MSCs starting by day 7; however, no increase for UC MSCs was detected. Higher OPN expression at day 14 in PP MSCs may also support the hypothesis of an earlier differentiation capacity in PP MSCs.

OTC and OPN mRNA and protein are expressed by only limited subsets of osteoblasts, depending on their maturational state and the microenvironment in which they reside.[33]

Given this fact, the variations we noted in OPN and OTC expression levels may be accounted for because the MSCs from both sources are not in synchronized cultures; they exist as a mix of osteoblasts in various states of differentiation. In addition, the NMF may generate microenvironments that further influence the generation of OTC and OPN. This could be related to NMF degradation patterns, which we are currently studying.

In order to lay the foundation for pre-clinical studies to test UC MSC-bone forming capacity in vivo, we have developed an autologous treatment algorithm in a juvenile swine model. Swine umbilical cords are harvested at birth using an explant technique similar to that performed in humans. The swine are identified, weaned at 3 weeks of age, acclimated for two weeks at the North Carolina School of Veterinary Medicine large animal facility, then undergo survival surgery. A critical sized maxillary defect is created, and treated with autologous UC MSCs on the PLGA scaffolds utilized in this study. Our initial data suggests that we are able to successfully generate bone within this defect.

In conclusion, both UC and PP MSCs attach, proliferate, and undergo osteogenic differentiation on Stryker® resorbable Delta System™ NMFs. The PLGA NMFs appear to have a greater trophic effect on the more primitive, less osteogenically committed, UC MSCs. Because NMF scaffolds allow earlier osteogenesis with matrix deposition, this may allow earlier implantation of tissue engineered constructs with potentially shorter times for healing of bone defects. The added benefit is that the UC is a discarded tissue, readily available at birth, simultaneous to the diagnosis of the craniofacial bone defect, and requires no secondary procedure for harvest.

Acknowledgments

Funding: These studies were made possible by funding through a grant from the Stryker® Craniomaxillofacial Corporation and through a KL2 Career Development Grant through the CTSA, 5KL2RR025746-03.

The Delta™ polymer used to create the PLGA nanofibers was donated generously by the Stryker® Craniomaxillofacial Corporation.

References

1. Woolley EJ, Richardson D, May P. Management of craniofacial abnormalities. Hosp Med. 2005; 66:405–10. [PubMed: 16025797]
2. Warschausky S, Kay JB, Buchman S, Halberg A, Berger M. Health-Related Quality of Life in Children with Craniofacial Anomalies. Plastic and Reconstructive Surgery. 2002; 110:409–14. [PubMed: 12142651]
3. Silber JS, Anderson DG, Daffner SD, Brislin BT, Leland JM, Hilibrand AS, et al. Donor Site Morbidity After Anterior Iliac Crest Bone Harvest for Single-Level Anterior Cervical Discectomy and Fusion. Spine. 2003; 28:134–9. [PubMed: 12544929]
4. Artico M, Ferrante L, Pastore FS, Ramundo EO, Cantarelli D, Scopelliti D, et al. Bone autografting of the calvaria and craniofacial skeleton: historical background, surgical results in a series of 15 patients, and review of the literature. Surgical Neurology. 2003; 60:71–9. [PubMed: 12865021]
5. Witsenburg B, Freihofer HPM. Autogenous rib graft for reconstruction of alveolar bone defects in cleft patients: Long term follow-up results. Journal of Cranio-Maxillofacial Surgery. 1990; 18:55–62. [PubMed: 2312739]
6. Warren SM, Fong KD, Chen CM, Loboa EG, Cowan CM, Lorenz HP, et al. Tools and Techniques for Craniofacial Tissue Engineering Tissue Engineering. 2004; 9:12.

7. Fong KD, Nacamuli RP, Song HM, Warren SM, Lorenz HP, Longaker MT. New Strategies for Craniofacial Repair and Replacement: A Brief Review. Journal of Craniofacial Surgery. 2003; 14:333–9. [PubMed: 12826804]
8. Susarla SM, Swanson E, Gordon CR. Craniomaxillofacial reconstruction using allotransplantation and tissue engineering: challenges, opportunities, and potential synergy. Ann Plast Surg. 2011; 67:655–61. [PubMed: 21825966]
9. Goldberg M, Langer R, Jia X. Nanostructured materials for applications in drug delivery and tissue engineering. J Biomater Sci Polym Ed. 2007; 18:241–68. [PubMed: 17471764]
10. van Aalst JA, Reed CR, Han L, Andrady T, Hromadka M, Bernacki S, et al. Cellular Incorporation Into Electrospun Nanofibers: Retained Viability, Proliferation, and Function in Fibroblasts. Annals of Plastic Surgery. 2008; 60:577–83.10.1097/SAP.0b013e318168db3e [PubMed: 18434835]
11. Reed CR, Han L, Andrady A, Caballero M, Jack MC, Collins JB, et al. Composite Tissue Engineering on Polycaprolactone Nanofiber Scaffolds. Annals of Plastic Surgery. 2009; 62:505–12.10.1097/SAP.0b013e31818e48bf [PubMed: 19387150]
12. Zhang Y, Lim C, Ramakrishna S, Huang Z-M. Recent development of polymer nanofibers for biomedical and biotechnological applications. Journal of Materials Science: Materials in Medicine. 2005; 16:933–46. [PubMed: 16167102]
13. Zhao X, Zhang S. Designer Self-Assembling Peptide Materials. Macromolecular Bioscience. 2007; 7:13–22. [PubMed: 17225214]
14. Nisbet DR, Forsythe JS, Shen W, Finkelstein DI, Horne MK. Review Paper: A Review of the Cellular Response on Electrospun Nanofibers for Tissue Engineering. Journal of Biomaterials Applications. 2008
15. Ushiki T. Collagen fibers, reticular fibers and elastic fibers. A comprehensive understanding from a morphological viewpoint. Archives of histology and cytology. 2002; 65:109–26. [PubMed: 12164335]
16. Imola MJ, Hamlar DD, Shao W, Chowdhury K, Tatum S. Resorbable Plate Fixation in Pediatric Craniofacial Surgery. Archives of Facial Plastic Surgery. 2001; 3:79–90. [PubMed: 11368657]
17. Taghizadeh RR, Cetrulo KJ, Cetrulo CL. Wharton's Jelly stem cells: Future clinical applications. Placenta. 2011; 32(Supplement 4):S311–S5. [PubMed: 21733573]
18. Can A, Karahuseyinoglu S. Concise Review: Human Umbilical Cord Stroma with Regard to the Source of Fetus-Derived Stem Cells. STEM CELLS. 2007; 25:2886–95. [PubMed: 17690177]
19. Gimble JM, Katz AJ, Bunnell BA. Adipose-Derived Stem Cells for Regenerative Medicine. Circulation Research. 2007; 100:1249–60. [PubMed: 17495232]
20. Soltan M, Smiler D, Soltan C. The Inverted Periosteal Flap: A Source of Stem Cells Enhancing Bone Regeneration. Implant Dentistry. 2009; 18:373–9.10.1097/ID.0b013e3181b9d7df [PubMed: 22129954]
21. Malizos KN, Papatheodorou LK. The healing potential of the periosteum: Molecular aspects. Injury. 2005; 36:S13–S9. [PubMed: 16188544]
22. Ringe J, Leinhase I, Stich S, Loch A, Neumann K, Haisch A, et al. Human mastoid periosteum-derived stem cells: promising candidates for skeletal tissue engineering. Journal of tissue engineering and regenerative medicine. 2008; 2:136–46. [PubMed: 18383554]
23. Caballero M, Reed CR, Madan G, van Aalst JA. Osteoinduction in Umbilical Cord- and Palate Periosteum-Derived Mesenchymal Stem Cells. Annals of Plastic Surgery. 2010; 64:605–9.10.1097/SAP.0b013e3181ce929 [PubMed: 20395805]
24. Rasband, WS. ImageJ. U. S. National Institutes of Health; Bethesda, Maryland, USA: 1997. http://rsbinfonihgov/ij/
25. Dominici M, Le Blanc K, Mueller I, Slaper-Cortenbach I, Marini F, Krause D, et al. Minimal criteria for defining multipotent mesenchymal stromal cells. The International Society for Cellular Therapy position statement. Cytotherapy. 2006; 8:315–7. [PubMed: 16923606]
26. Bakhshi T, Zabriskie RC, Bodie S, Kidd S, Ramin S, Paganessi LA, et al. Mesenchymal stem cells from the Wharton's jelly of umbilical cord segments provide stromal support for the maintenance of cord blood hematopoietic stem cells during long-term ex vivo culture. Transfusion. 2008; 48:2638–44. [PubMed: 18798803]

27. Jo C, Kim O-S, Park E-Y, Kim B, Lee J-H, Kang S-B, et al. Fetal mesenchymal stem cells derived from human umbilical cord sustain primitive characteristics during extensive expansion. Cell and Tissue Research. 2008; 334:423–33. [PubMed: 18941782]

28. Chen X-D, Qian H-Y, Neff L, Satomura K, Horowitz MC. Thy-1 Antigen Expression by Cells in the Osteoblast Lineage. Journal of Bone and Mineral Research. 1999; 14:362–75. [PubMed: 10027901]

29. Kaspar D, Seidl W, Neidlinger-Wilke C, Beck A, Claes L, Ignatius A. Proliferation of human-derived osteoblast-like cells depends on the cycle number and frequency of uniaxial strain. Journal of Biomechanics. 2002; 35:873–80. [PubMed: 12052389]

30. Ball MD, Bonzani IC, Bovis MJ, Williams A, Stevens MM. Human periosteum is a source of cells for orthopaedic tissue engineering: a pilot study. Clinical orthopaedics and related research. 2011; 469:3085–93. [PubMed: 21547415]

31. Characterization of human embryonic stem cell lines by the International Stem Cell Initiative. Nat Biotech. 2007; 25:803–16.

32. Riekstina U, Cakstina I, Parfejevs V, Hoogduijn M, Jankovskis G, Muiznieks I, et al. Embryonic Stem Cell Marker Expression Pattern in Human Mesenchymal Stem Cells Derived from Bone Marrow, Adipose Tissue, Heart and Dermis. Stem Cell Reviews and Reports. 2009; 5:378–86. [PubMed: 20058201]

33. Aubin JE. Regulation of osteoblast formation and function. Reviews in endocrine & metabolic disorders. 2001; 2:81–94. [PubMed: 11704982]

34. Owen TA, Aronow M, Shalhoub V, Barone LM, Wilming L, Tassinari MS, et al. Progressive development of the rat osteoblast phenotype in vitro: reciprocal relationships in expression of genes associated with osteoblast proliferation and differentiation during formation of the bone extracellular matrix. Journal of cellular physiology. 1990; 143:420–30. [PubMed: 1694181]

35. Jang W-G, Kim E-J, Kim D-K, Ryoo H-M, Lee K-B, Kim S-H, et al. BMP2 Protein Regulates Osteocalcin Expression via Runx2-mediated Atf6 Gene Transcription. Journal of Biological Chemistry. 2012; 287:905–15. [PubMed: 22102412]

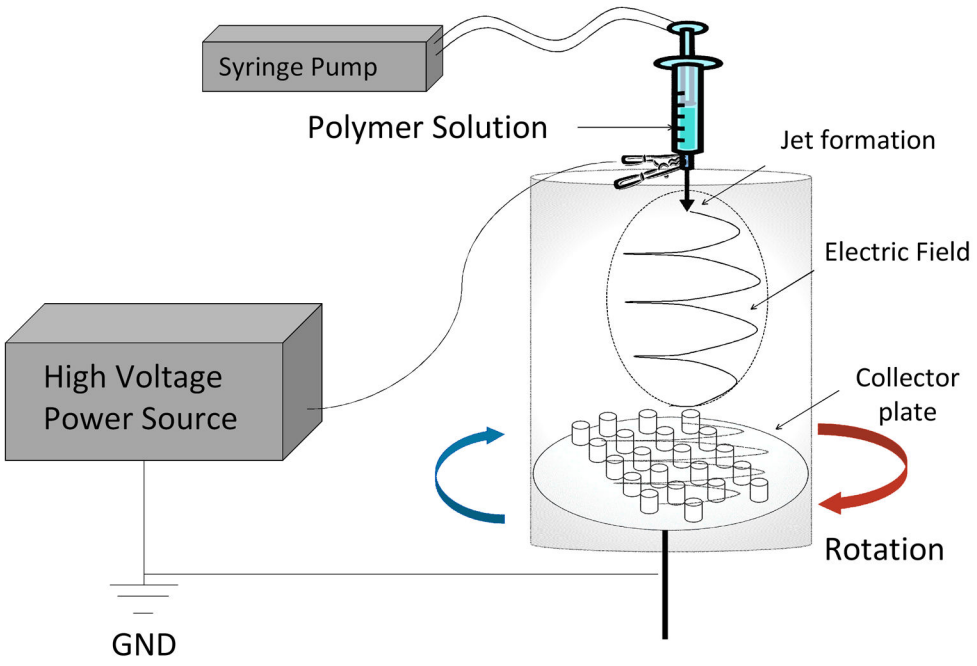

Figure 1.

Electrospinning apparatus. The electrospinning apparatus consists of a syringe attached to a pump, which directs a viscous polymer across a voltage potential toward a collecting plate. When the voltage potential overcomes the surface tension of the viscous polymer, the polymer jet is directed toward the collecting plate where the fibers dry. Fiber diameters and porosities (related to the density of the fiber mat) are controlled by polymer choice and viscosity, diameter of the syringe needle, voltage potential, and distance to the collecting plate.

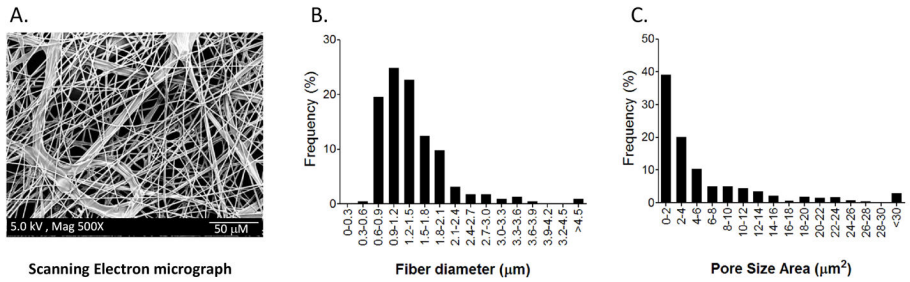

Figure 2.

Nanomicrofiber (NMF) characterization. Poly-co-glycolytic acid (PLGA) fibers were electrospun using standard techniques. Scanning electron micrographs (SEM) of these NMF mats were obtained. Representative micrographs suggest that PLGA fibers and are a mixture of fiber diameters (A). PLGA fiber diameters and porosities were measured by SEM; fibers ranged from 0.6 to 2.1 µm in diameter (B) and pore sizes are within a 0 to 6 µm range (C).

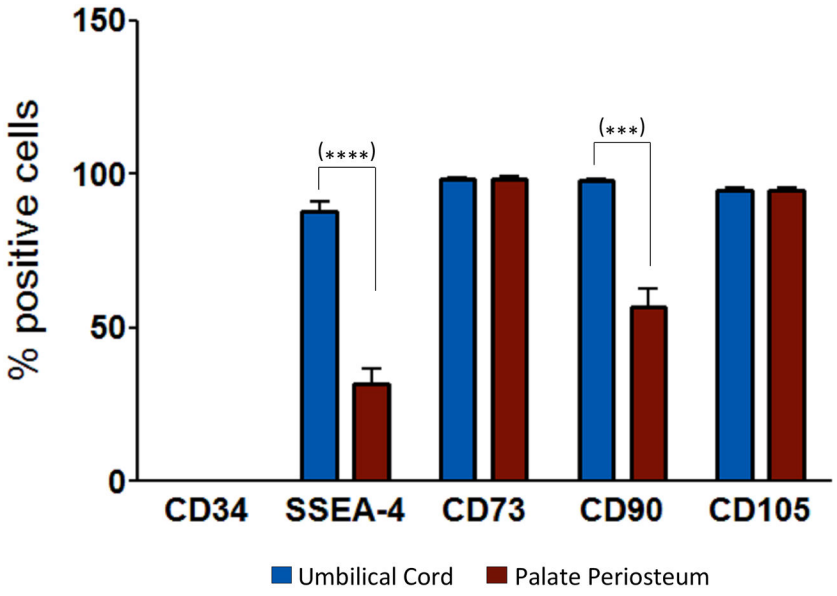

	CD34	SSEA-4	CD73	CD90	CD105
UC	0	88	98	98	95
PP	0	32	98	57	95

Figure 3.

Mesenchymal stem cell (MSC) surface markers. Standard markers were determined for MSCs harvested from Umbilical Cord (UC) (n = 6) and Palate Periosteum (PP) (n = 5) sources using flow cytometry. All cells were negative for CD 34, a hematopoietic stem cell marker, and positive for SSEA-4 (a primitive cell surface marker), CD 73, CD 90, and CD 105. Data are reported as the mean percentage of positive cells ± standard error of the mean. Statistical analysis was performed using a double tailed, pair wise t-test. SSEA-4 ($P \leq 0.001$; ***) and CD 90 ($P \leq 0.0001$; ****) were statistically higher in UC MSCs.

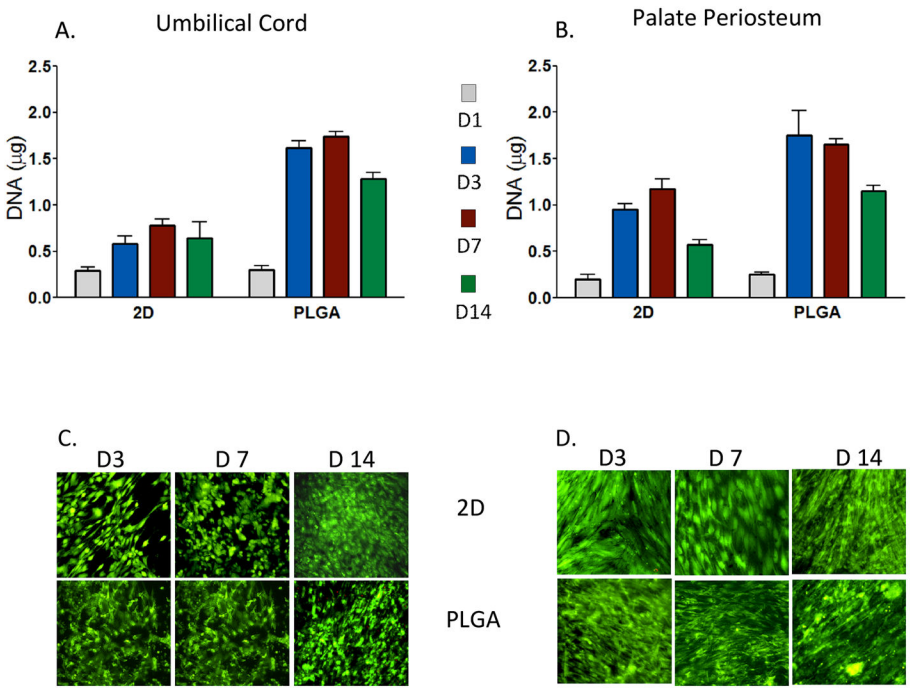

Figure 4.

Mesenchymal Stem cells (MSC) proliferation and viability. Cell proliferation and viability in Umbilical Cord (UC) and Palate periosteum (PP) MSCs (n = 4) seeded onto 2D surfaces and PLGA fibers were assessed at days 1, 3, 7, 14, and 21 post-differentiation. Cell proliferation was measured by DNA quantification for UC (A) and PP (B). Data were reported as the mean total DNA in μg ± standard error of the mean. Statistical significance was designated as $P < 0.05$ (*); no statistically significant differences were noted between the conditions. Viability was qualitatively measured by Calcein AM staining; representative pictures for UC (C) and PP (D) are shown. PLGA scaffolds supported proliferation sooner and to a greater degree in MSCs from both sources.

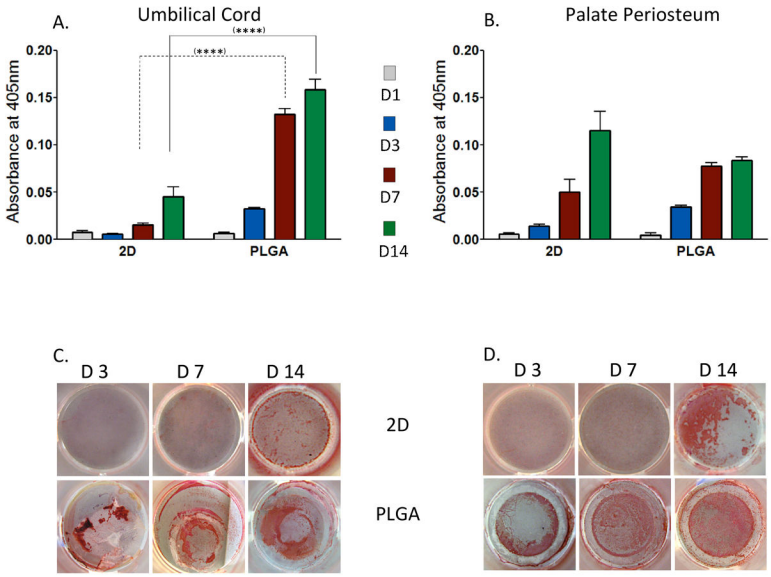

Figure 5.

Calcium deposition measured by Alizarin Red staining. Umbilical cord (UC)- and palate periosteum (PP)-mesenchymal stem cells (MSC) (n=3) were osteoinduced on 2D and PLGA scaffolds; alizarin red staining for calcium deposition was assessed at days 1, 3, 7, and 14. Calcium deposition was noted sooner (by day 7; A and C) and more sustained (at day 14) in UC MSCs on PLGA scaffolds ($p < 0.0001$; ****). Calcium deposition was more pronounced in PP-MSCs on PLGA scaffolds on days 3 and 7, but greater on 2D surfaces by day 14 (B and D; without statistical significance). Statistical significance is reported as $P \geq 0.05$ (ns), $P < 0.05$ (*), $P \leq 0.01$ (**), $P \leq 0.001$ (***), $P \leq 0.0001$ (****).

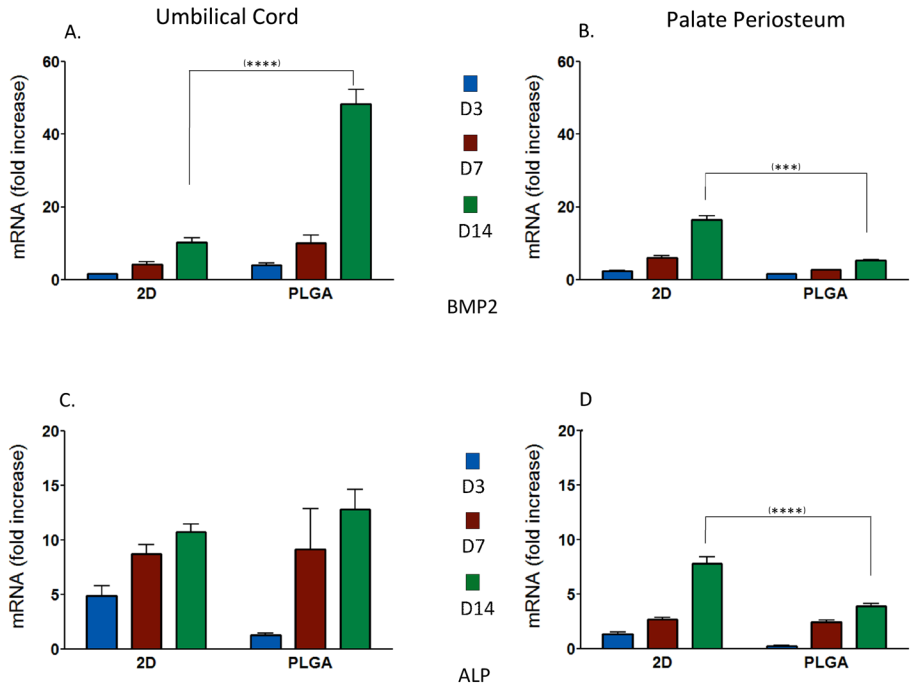

Figure 6.

Early markers of osteoinduction. Following osteoinduction of both umbilical cord (UC)- and palate periosteum (PP-derived MSCs (n=5), mRNA for bone morphogenetic protein 2 (BMP2) (A, B) and alkaline phosphatase (ALP) (C, D) were assessed using RT-PCR. Fold-increase in mRNA is recorded on the y-axis. BMP2 mRNA levels were higher in PLGA for UC-MSCs at all time points (A), with statistical significance at day 14 ($p \leq .0001$; ****) while no difference was noted for ALP. For PP-MSCs, both BMP2 and ALP were higher in 2D surfaces (B, D). Data were reported as the $2^{-\Delta\Delta CT}$ mean ± standard error of the mean. Statistical significance is reported as $P \geq 0.05$ (ns), $P < 0.05$ (*), $P \leq 0.01$ (**), $P \leq 0.001$ (***), $P \leq 0.0001$ (****).

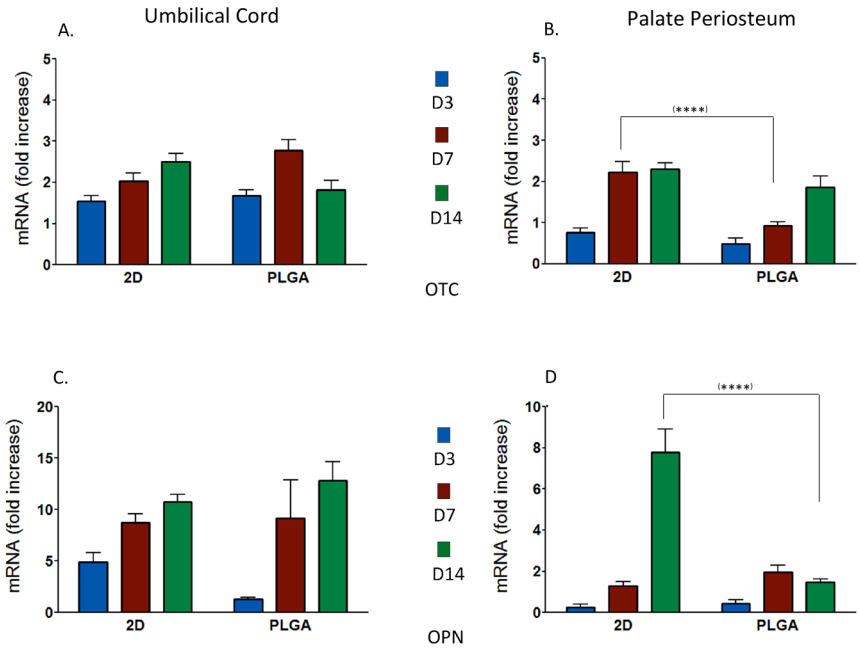

Figure 7.

Late markers of osteoinduction. Following osteoinduction of both UC and PP-MSCs (n=5), mRNA for OTC (A, B) and OPN (C, D) was assessed using RT-PCR. Fold-increase in mRNA is recorded on the y-axis. OTC and OPN mRNA levels were similar in 2D and PLGA for UC (A, C) through day 14. For PP-MSCs OTC and OPN levels are higher in 2D than PLGA (B, D). Data were reported as the $2^{-\Delta\Delta CT}$ mean ± standard error of the mean. Statistical significance is reported as $P \geq 0.05$ (ns), $P < 0.05$ (*), $P \leq 0.01$ (**), $P \leq 0.001$ (***), $P \leq 0.0001$ (****).

Table 1

Primers and probes used for real time quantitative-PCR.

BMP2	
Forward	CCA GAC CAC CGG TTG GAG A
Reverse	TTC CAA AGA TTC TTC ATG GTG G G
Probe	FAG CCA GCC GAG CCA ACA CTG TGC Q
ALPL	
Forward	CCC CGT GGC AAC TCT ATC TT
Reverse	CCA TAC AGG ATG GCA GTG AA
Probe	FCT GGC CCC CAT GCT GAG TGA CAC AQ
OTC	
Forward	GTG GAG GAG CTG CAG CTA CA
Reverse	ACC AGC TCC CTC TGT TCT CT
Probe	FAG GCC CAG CAG CAG GCC TG GG CA Q
OPN	
Forward	AGT TTC GCA GAC CTG ACA TC
Reverse	TCA ACT CCT CGC TTT CCA TG
Probe	FTA CCC TGA TGC TAC AGA CGA GGA CQ
18S	
Forward	CCA GAC CAC CGG TTG GAG A
Reverse	TTC CAA AGA TTC TTC ATG GTG G G
Probe	FAG CCA GCC GAG CCA ACA CTG TGC Q

F; 5′-Fluorescein (FAM) and 5′-Tetrachloro-Fluorescein (TET) in 18S.

Q; Quencher (TAMRA)

Table 2

Quantification of umbilical cord (UC) and palate periosteum (PP) mesenchymal stem cells (MSC) proliferation and calcification. The differences between mean total DNA values (proliferation) and mean absorbance values after staining with Alizarin Red at 405 nm (calcification) for UC- compared to PP-MSCs (n=5) are reported. The designation UC > PP indicates a higher proliferation and calcium deposition in UC when compared to PP MSCs; while UC < PP indicates a decrease. Proliferation was generally greater in UC than PP MSCs on both 2D and PLGA conditions. Calcium deposition was higher in UC-MSCs than PP-MSC on PLGA scaffolds beginning on day 7 (with statistical significance).

Umbilical Cord MSC compared to Palate Periosteum MSC				
	2D		**PLGA**	
Days	**Difference**	**Significance**	**Difference**	**Significance**
PROLIFERATION				
D1	UC>PP	ns	UC=PP	ns
D3	UC>PP	ns	UC>PP	ns
D7	**UC>PP**	**P<0.05**	UC>PP	ns
D14	UC>PP	ns	UC<PP	ns
CALCIFICATION				
D1	UC=PP	ns	UC=PP	ns
D3	UC=PP	ns	UC=PP	ns
D7	UC<PP	ns	**UC>PP**	**P ≤ 0.01**
D14	**UC<PP**	**P ≤ 0.01**	**UC>PP**	**P ≤ 0.0001**

Ann Plast Surg. Author manuscript; available in PMC 2015 June 01.

Table 3

Bone morphogenetic protein 2 (BMP2), alkaline phospatase (ALP), Osteocalcin (OTC) and osteopontin (OPN) mRNA comparisons between umbilical cord (UC) and palate periosteum (PP) mesenchymal stem cells (MSCs). BMP2 levels were higher in PP- than UC-MSCs on 2D surfaces. However, on PLGA nano-microfibers, UC-MSCs demonstrated higher BMP2 levels (with statistical significance at day 14). ALP expression was generally higher in UC- than PP-MSC conditions, with the 2D conditions at day 7 and 14 demonstrating statistical significance. Data was obtained by statistical comparison of the mean total from the $2^{-\Delta\Delta CT}$ mean values. Statistical significance is reported, with ns indicating a lack of statistical significance ($P \geq 0.05$).

Umbilical Cord MSC compared to Palate Periosteum MSC				
	2D		**PLGA**	
Days	**Difference**	**Significance**	**Difference**	**Significance**
BMP2				
D3	UC<PP	ns	UC>PP	ns
D7	UC<PP	ns	UC>PP	ns
D14	UC<PP	ns	**UC>PP**	**P ≤ 0.0001**
ALP				
D3	UC>PP	ns	UC<PP	ns
D7	**UC<PP**	**P ≤ 0.001**	UC>PP	ns
D14	**UC>PP**	**P ≤ 0.0001**	UC>PP	ns
OTC				
D3	UC>PP	ns	UC>PP	ns
D7	UC<PP	ns	**UC>PP**	**P ≤ 0.001**
D14	UC>PP	ns	UC<PP	ns
OPN				
D3	UC>PP	ns	UC>PP	ns
D7	UC>PP	ns	UC<PP	ns
D14	UC<PP	ns	UC>PP	ns

Ann Plast Surg. Author manuscript; available in PMC 2015 June 01.